Remote Sensing of Environment 123 (2012) 496–507

Contents lists available at SciVerse ScienceDirect

Remote Sensing of Environment

journal homepage: www.elsevier.com/locate/rse

Estimating surface soil moisture over Sahel using ENVISAT radar altimetry

C. Fatras *, F. Frappart, E. Mougin, M. Grippa, P. Hiernaux

Université de Toulouse, OMP, GET (UMR 5563 CNRS-UPS-IRD), 14 avenue Edouard Belin 31400 Toulouse, France

ARTICLE INFO

Article history:
Received 18 November 2011
Received in revised form 7 March 2012
Accepted 19 April 2012
Available online xxxx

Keywords:
Surface soil moisture
Radar altimetry
Backscattering coefficient
Sahel

ABSTRACT

This paper analyzes the potential of the radar altimeter onboard ENVISAT for estimating surface soil moisture in the semi-arid Gourma region in Northern Mali. To this end, the relationships between observed backscattering coefficients derived from 4 retracking algorithms, namely Ocean, Ice-1, Ice-2 and Sea-Ice, and ground data, including soil type, topography, vegetation and soil moisture are investigated. The considered period is 2002–2010. Results show a strong linear relationship between the backscattering coefficients and surface soil moisture measured at six different stations along the satellite track. The best results are obtained with the Ice-1 and Ice-2 algorithms. In these cases, correlation coefficients are higher than 0.8 with RMSE smaller than 2%. Vegetation effects are found to be small due both to the nadir-looking configuration of the radar altimeter and to the low vegetation cover. Finally, the relationship between soil moisture and normalized backscattering coefficient is used to retrieve soil moisture from the altimeter data. These estimates are then compared to soil moisture estimations obtained from the METeorological Operational (METOP) Advanced SCATterometer (ASCAT). These results highlight the high capabilities of Ku-band altimeters to provide an accurate estimation of surface soil moisture in semiarid regions.

1. Introduction

In the Sahelian region of West-Africa, soil moisture drives many surface processes including soil organic matter mineralization (e.g. Zech et al., 1997), vegetation productivity (e.g. Hiernaux et al., 2009), land surface fluxes (e.g. Brümmer et al., 2008) and land surface–atmosphere interactions (e.g. Taylor et al., 2010). Particularly, the Sahel is identified as one of the regions of the world with the strongest feedbacks between soil moisture and precipitation (Koster et al., 2004). Monitoring of the spatio-temporal variability of soil moisture is therefore an important issue within the frame of the AMMA (*African Monsoon Multidisciplinary Analysis*) project which aims at providing a better understanding of the West African Monsoon and its physical, chemical and biological environments (Redelsperger et al., 2006).

Active microwave remote sensing has demonstrated considerable capabilities in estimating surface soil moisture (SSM), in semi-arid regions (e.g. Mladenova et al., 2010; Wagner & Scipal, 2000). The potential of radar sensors for detecting changes in SSM results from their high sensitivity to the variation of surface dielectric properties that are mainly linked to changes in SSM. Moreover, in semi-arid regions, observations made at low incidence angles are found to be strongly correlated to SSM because vegetation effects are minimized (Baup et al., 2007; Moran et al., 2000; Tansey et al., 1999).

Initially designed to make accurate measurements of the sea surface topography, satellite radar altimetry (RA) has been successfully employed to derive valuable information for land hydrology by providing an estimation of water level variations of lakes (Birkett, 1995; Cazenave et al., 1997; Crétaux et al., 2009), rivers (Birkett, 1998; Birkett et al., 2002; Frappart et al., 2006a) and floodplains (Frappart et al., 2005, 2006b; Santos da Silva et al., 2010). The magnitude of RA backscattering coefficients σ_0 provided by the TOPEX/POSEIDON altimeter mission at Ku- and C-bands, and by the European ENVIronmental SATellite (ENVISAT), at Ku and S bands, is related to the dynamics of surface properties (e.g. Legrésy et al., 2005; Papa et al., 2003). Particularly, spatial and temporal variations of RA backscattering coefficients are found to be related to soil roughness and surface soil moisture (SSM) changes in the Sahara and Australian deserts (Cudlip et al., 1994; Ridley et al., 1996). Moreover, a semi-empirical model was recently proposed to estimate SSM using RA backscattering coefficients over semi-arid surfaces (Bramer et al., 2010). Comparisons were made with soil moisture outputs from a hydrological model showing a link between modeled and altimetry derived soil moisture. Radar altimeters are a priori suitable to SSM retrieval since attenuation by the vegetation layer is minimized by their nadir-looking configuration. This is particularly true in semi-arid regions where vegetation cover is sparse. However, their potentials for SSM retrieval have not been demonstrated yet.

The objective of the present study is to investigate whether the backscattering coefficient delivered by radar altimetry can be used to provide an accurate estimation of surface soil moisture over semi-arid areas. To this end, the data acquired by the ENVISAT RA-2

* Corresponding author at: Géosciences Environnement Toulouse (GET), Observatoire Midi-Pyrénées, 14 avenue Edouard Belin 31400 Toulouse, France.
E-mail address: christophe.fatras@get.obs-mip.fr (C. Fatras).

0034-4257/$ – see front matter © 2012 Elsevier Inc. All rights reserved.
doi:10.1016/j.rse.2012.04.013

over Northern Sahel in Mali are analyzed over the 2002–2010 period and relationships are investigated between observed backscattering coefficients and ground data including soil type, topography, vegetation and soil moisture acquired at six different stations along the satellite track. For the sandy soils sites, a linear relationship is derived between the altimetry backscatter and the in situ SSM. Finally, this relationship is used to retrieve soil moisture from the altimeter data and the resulting soil moisture estimate is compared to the estimate obtained from the METeorological Operational (METOP) Advanced SCATterometer (ASCAT).

2. Study area and data

2.1. The study site

The African Monsoon Multi-disciplinary Analysis — Couplage de l'Atmosphère Tropicale et du Cycle Hydrologique (AMMA-CATCH) meso-scale site is located in the Gourma region (1°W–2°W, 14.5°N–17.5°N) in Mali (Fig. 1), and stretches from the loop of the Niger River southward down to the country border with Burkina-Faso (Mougin et al., 2009). This site is entirely located within the Sahel bioclimatic zone and is bracketed by the 150 and 500 mm annual isohyets. The rain distribution is strictly mono-modal with rainfall starting in June and ending in September with a maximum in August (Frappart et al., 2009). During the wet season, rangeland vegetation is composed of a low herbaceous layer dominated by annuals and a sparse woody plant population (canopy cover <5%). Annual herbs germinate with the first significant rains, in June or July, and unless the plants wilt before maturity owing to a lack of rainfall, the senescence coincides approximately with the end of the rainy season. This short rainy season is followed by a long dry season during which there is no green vegetation except for rare perennial herbaceous and the foliage of some of scattered trees and shrubs.

The Gourma region is a vast peneplain at between 250 and 330 m altitude with highest isolated sandstone buttes reaching 900–1100 m close to the town of Hombori. The eroded and exposed rock-surfaces (23% of the whole area) are locally capped by iron pan but larger areas of the region (58%) are covered by deep and fixed sand. At meso-scale, predominantly sandy or shallow soils distribute in large alternant swaths of contrasted land cover (Fig. 1). Besides these two major landforms, remnants of alluvial systems and lacustrine depressions form a web of narrow valleys often slotted in between sandy and shallow soils.

The overall observation strategy of the AMMA-CATCH site is based on the deployment of a variety of instrument networks, from local- to meso-scales, dedicated to the monitoring and documentation of the major variables characterizing the climate and the spatio-temporal variability of geophysical and land surface variables. Long term measurements monitor meteorological variables, vegetation and surface hydrology including soil moisture.

2.2. Surface soil moisture measurements

Six automatic soil moisture stations are located at the vicinity of the ENVISAT's path #302 (Fig. 1). These stations are part of the soil moisture network set up from 2005 within the frame of the AMMA project (de Rosnay et al., 2009). Characteristics (name, location, date of installation, soil type, sensor depth) of the 6 soil moisture stations are given in Table 1. The same installation protocol is used for all the soil moisture stations equipped by Time Domain Reflectometry sensors (Campbell Scientific CS616) that provide measurements at 15 min time step, except for the Eguerit erosion surface site where delta-T sensors have been installed. Sensors are calibrated by using in situ gravimetric measurements and estimation of soil bulk density. Only surface measurements recorded at 5, 10, 30 and 40 cm depth are considered here in agreement to the microwave soil penetration depth (Ulaby et al., 1981). In the following, Surface Soil Moisture (SSM) data are expressed in volumetric water content ($m^3\,m^{-3}$). Local SSM data typically range between 0.05% (dry season) and 28% (wet season) for the sandy soils.

2.3. ENVISAT RA-2 backscattering coefficients

In the framework of its Earth observation program, the European Space Agency (ESA) launched the ENVIronmental SATellite (ENVISAT) satellite on February 2002. ENVISAT carries 10 scientific

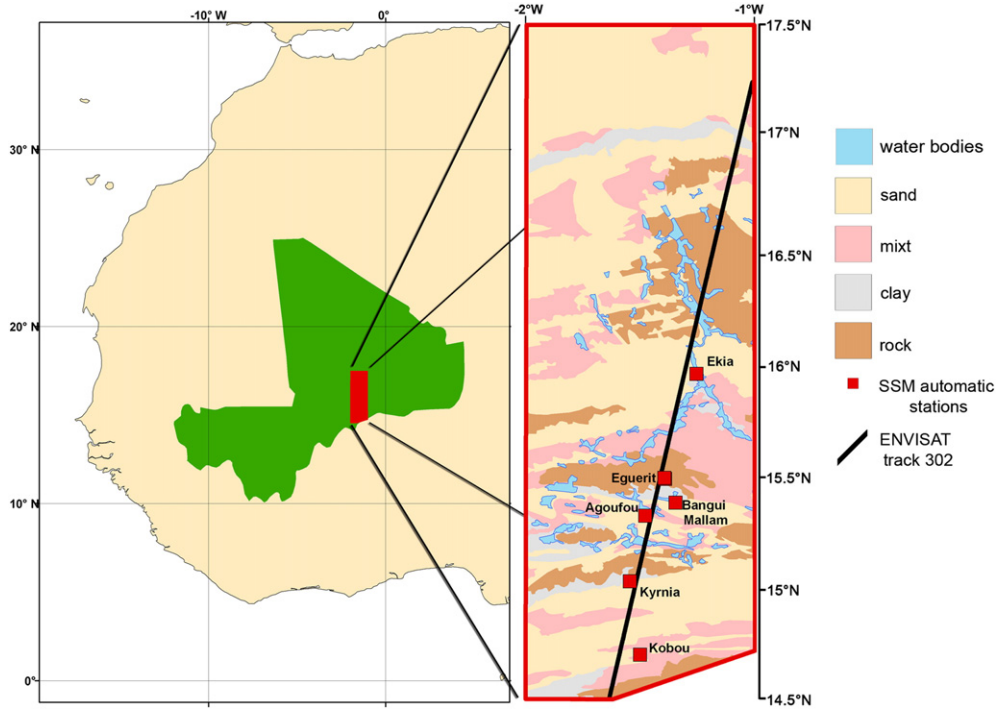

Fig. 1. The AMMA-CATCH mesoscale site in Mali, showing the 6 automatic soil moisture stations (squares) and ENVISAT path 302 (black line).

Table 1
Description of study sites and surface soil moisture (SSM) and precipitation data.

Site name		Agoufou	Bangui Mallam	Eguerit	Ekia	Kobou	Kyrnia
Latitude		15.3453°	15.3978°	15.5026°	15.9651°	14.7284°	15.051°
Longitude		−1.47913°	−1.34556°	−1.391°	−1.2534°	−1.502°	−1.546°
Soil type		Sand	Sand, clay	Rock	Sand	Sand, rock	Sand, clay
SSM	Period	2005–2010	2005–2010	2008–2009	2005–2010	2008–2010	2007–2010
	Depth (cm)	5, 10, 40	5[a], 10, 30	5	5, 10, 30	5, 10, 30	5, 10, 30
	Resolution (min)	15	15	15	15	15	15
Rain gauge	Period	2005–2010	2005–2010	2008–2009	2005–2010	2005–2010	2005–2009
	Resolution (min)	5	5	5	5	5	5

[a] Measurements at 5 cm are only available during the 2005–2008 period.

instruments which provide atmosphere, ocean, land, and ice measurements, including a nadir-pointing radar altimeter (RA-2 or Advanced Radar Altimeter) (Wehr & Attema, 2001). ENVISAT flies in a sun-synchronous polar orbit at an altitude of about 800 km, with a 35-day repeat cycle and an inclination of 98.6°, providing observations of the Earth surface (ocean and land) from 81.5° latitude North to 81.5° latitude South, with a ground-track spacing of around 80 km at the Equator. RA-2 is a nadir-looking pulse-limited radar altimeter operating at two frequencies at Ku- (13.575 GHz/2.3 cm of wavelength) and S- (3.2 GHz/9.3 cm) bands (Zelli, 1999). Its main characteristics are summarized in Table 2. The diameters of the pulse-limited footprint are respectively 3.4 km in Ku and 4.8 km in S bands (ESA, 2002). However, the surface footprint size is uncertain and its nominal diameter varies approximately between 2 km and 10 km for Ku band (Chelton et al., 2001; Peacock & Laxon, 2004). These variations are caused by the topography and the inhomogeneities of the surface. Over flat surfaces, an approximate radius of 2 km is generally considered as a good approximation for Ku band (Chelton et al., 2001). Over land, the presence of open water in the footprint produces strong specular reflections that can be off-nadir. The returned signal can be dominated by these off-nadir reflections causing tracking errors (altimeter mispointing) even if they are off-nadir by several (1–10) km for Ku band, and beyond for S band due to a larger beam width. Processing of radar echoes or altimeter waveforms is performed on the ground to obtain range values, i.e. the distance between the satellite and the surface estimated from the round-trip time of the electromagnetic pulse, and backscattering coefficients σ_0 derived from the power of the altimeter return pulse. The Geophysical Data Records (GDRs) distributed by ESA (ESA, 2002) include accurate satellite positions (longitude, latitude and altitude of the satellite on its orbit) and timing, altimeter ranges, instrumental, propagation and geophysical corrections applied to the range, and several other parameters such as the backscattering coefficients. For the ENVISAT mission, four different retracking algorithms are operationally applied to RA-2 raw-data to provide range estimates and backscattering coefficients. Each retracking algorithm namely Ocean (Brown, 1977; Hayne, 1980), Ice-1 (Bamber, 1994; Wingham et al., 1986), Ice-2 (Legrésy, 1995; Legrésy & Rémy, 1997) and Sea-Ice (Laxon, 1994) has been developed for a specific type of surface but none of them has been specifically designed for processing altimeter echoes over land. The backscattering coefficient is directly related to the integral against time of the radar echo or waveform. Ocean and Ice-2 algorithms are based on the fit of a theoretical waveform shape corresponding to sea and ice cap surfaces to estimate precisely the position of the leading front of the waveform. The value of the backscattering coefficient is determined by integration of the theoretical waveform. For Ice-1 and Sea Ice these parameters are estimated empirically using thresholds on the amplitude of the waveform. The errors on the estimated σ_0 (instrument noise, orbit variations, atmosphere interferences) are expected to be lower than 0.29 dB in Ku band and 0.37 dB in S band (Pierdicca et al., 2006).

The variables used in this study, include the satellite positions, times of acquisition, the 1 Hz Ocean-retracked (Ku and S bands), the 18 Hz Ice-1, Ice-2 (Ku and S bands), and the 18 Hz Sea Ice (Ku band) backscattering coefficients contained in the ENVISAT RA-2 GDRs made available by the Centre de Topographie des Océans et de l'Hydrosphère (CTOH — http://ctoh.legos.obs-mip.fr/) for the ground track #302 over the AMMA mesoscale site in Gourma (see Fig. 1). The considered period is September 2002–October 2010 (8 years). However, S-band data are only available until January 2008 (5.4 years).

2.4. ASCAT SSM products

The METeorological Operational (METOP) Advanced SCATterometer (ASCAT) is the enhanced successor of the scatterometers flown on the European Remote Sensing (ERS-1 and ERS-2) satellites. ASCAT operates at C-band (5.255 GHz) with VV polarization. Two triplets of spatially averaged backscattering coefficient values at a spatial resolution of around 30 and 50 km for each location along the swath are derived from continuous observations performed by three radar antenna beams at three different azimuth angles (45°, 90°, and 135° sideward from the direction of the satellite motion) on both side of the METOP satellite (Naeimi et al., 2009). Technical information concerning ASCAT measurements are presented in Table 3. SSM products based on these observations are then generated using the SSM retrieving algorithm developed by Wagner (1998) from ERS data. The backscattering coefficients are first normalized to a

Table 2
ENVISAT RA-2 technical specifications.

Repeat cycle	35 days
Altitude	782.4–799.8 km
Emitted frequencies (GHz)	(Ku) 13.575–(S) 3.2
Antenna beam width (°)	(Ku) 1.29–(S) 5.5
Backscatter maximum error (dB)	(Ku) 0.29–(S) 0.37
Pulse-limited footprint diameter (km)	(Ku) 3.4–(S) 4.8
Swath dispersion (km)	2

Table 3
ASCAT technical specifications.

Altitude	~822 km
Emitted frequencies (GHz)	5.255
Incidence angles	25° to 65°
Spatial resolution	50 km
Nodal grid	25 km
Orbit cycle	29 days
Accuracy of SSM products	0.04–0.08 m^3m^{-3}
Data availability over Gourma	Daily

standard incidence of 40°, and then inverted into SSM assuming a linear relationship between these two quantities. In this study, we use the interpolated SSM products given at a resolution of 30 km following a nodal grid of 12.5 km, which correspond to the closest time to the altimetry measurements (with a variation from a few minutes to 18 h), for the period June 2007–October 2010.

3. Spatio-temporal variations of RA-2 backscattering coefficients

Along-track profiles (Fig. 2) of σ_0 in Ku- and S-bands are averaged at each satellite pass at a spatial resolution of 0.008° (~1 km) for the rainy (JJAS) and the core of the dry (JFMA) seasons for Ocean, Ice-1, Ice-2, and Sea Ice retracking algorithms over the ENVISAT RA-2

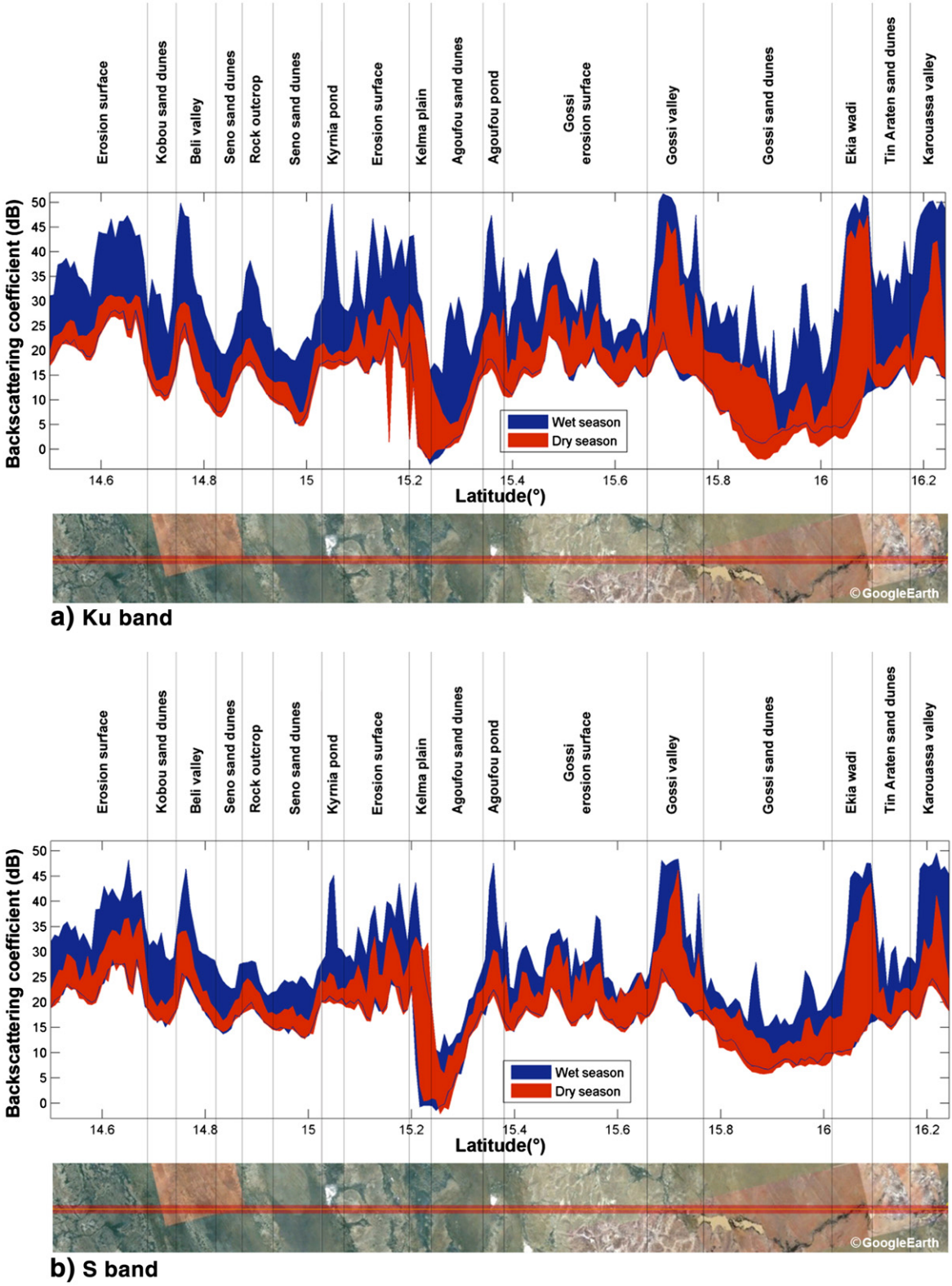

Fig. 2. Spatial variations of the backscattering coefficient along the ENVISAT RA-2 groundtrack 302 for dry (January–April) and wet (JJAS) seasons using Ice-1 algorithm. a) Ku band; b) S band. Image from Google-Earth is shown for comparison.

groundtrack #302 between latitudes 14.5° and 16.25°. This spatial resolution is chosen as it captures the spatial heterogeneity of the surface (Mougin et al., 2009) and of the local soil moisture condition (Baup et al., 2007; de Rosnay et al., 2009). It corresponds to three different 18 Hz measurements which footprint centers are separated by 370 m for Ice-1, Ice-2, and Sea Ice σ_0, and one 1 Hz measurements (corresponding to a distance of 7.5 km) for Ocean σ_0.

In the following, only the results obtained with the Ice-1 retracking algorithm are displayed. Results using the three other retracking algorithms are cited and discussed in the text.

3.1. Backscattering coefficient seasonal variations along the latitudinal transect

The extreme values reached per grid cell over the whole observation periods by σ_0 for Ku-band (8 years) and S-band (5.4 years) are identified for the Ice-1 processing during the wet seasons (June to September) and the core of the dry season (January to April). Similar profiles are obtained for Ku and S bands with a lower dynamics for the S band in general, especially over sandy areas. The spatial σ_0 dynamics during the dry season is slightly larger for S-band than for Ku-band. On the contrary, the spatial dynamics during the wet season is lower for S-band than for Ku-band. This can be due both to the larger footprint of S band that encompasses surfaces of different types (i.e., mix between rocky, sandy and clay soils, or presence of permanent ponds far from nadir that have a signature in S but not in Ku bands) and to a lower sensitivity of the S band (wavelength of 9 cm) to changes in surface roughness. Lower values of backscattering coefficients are generally observed over sandy surfaces (fixed dunes) whereas higher values are found over rocky surfaces (erosion surfaces) and surfaces containing temporary open water (ponds and wadi). The higher surface roughness of the sandy surfaces could account for a smaller backscattering response in the nadir direction. The yearly amplitude of the backscattered signal exhibits large variations along the latitudinal transect, from 10 to 30 dB for Ku-band and from 10 to 20 dB for S-band over sandy surfaces, from 15 to 30 dB for Ku-band and from 15 to 20 dB for S-band over erosion rocky surfaces, and reaches 45 dB over water bodies for both bands, as illustrated by the response of the Ekia wadi (16.05° N).

Similar along-track profiles are obtained with the other retracking algorithms. However the profiles established with Ocean are smoother as only 1 Hz data are available with this processing.

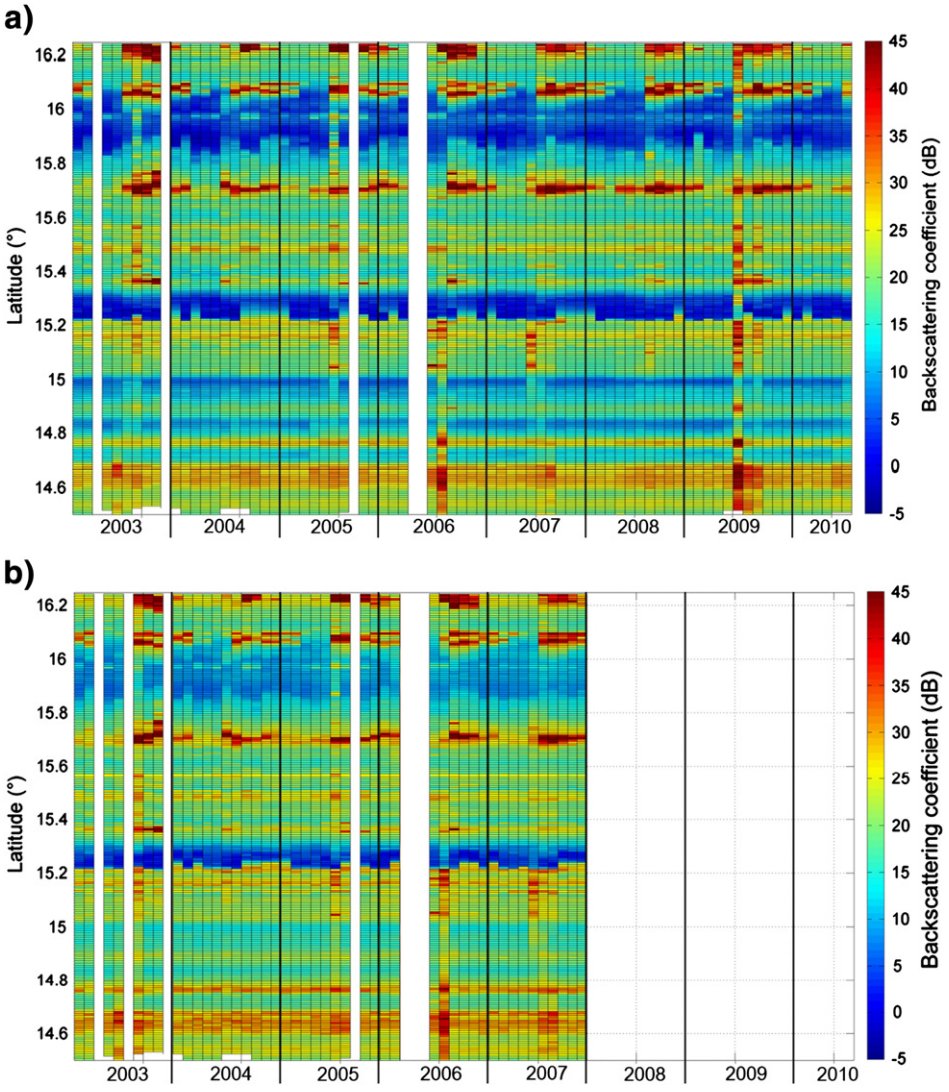

Fig. 3. Space-time diagram of ENVISAT RA-2 data over the AMMA-CATCH mesoscale window with Ice-1 backscattering coefficient values for a sampling rate in latitude of 0.008° (about 1 km). Blank stripes correspond to missing or corrupted values. a) Ku-band (2003-2010); b) S-band (2003-2007).

3.2. Spatio-temporal variations along the latitudinal transect

The latitudinal variations of the backscattering coefficient from the track #302 are plotted as a function of time over the 2003–2010 period for Ku-band (Fig. 3a) and over the 2003–2007 period for S-band (Fig. 3b). They both exhibit a well-marked seasonality with higher values of σ_0 during the rainy season, particularly at latitudes above 15.4°N where rocky soil types and ponds are more important. However, for the same type of surface, the values are generally higher in the South than in the North in agreement with the rainfall gradient (Frappart et al., 2009). During the wet season, three zones in the North (around 15.75°, 16.1° and 16.2° of latitude) present very strong backscattering coefficients at both frequencies. They correspond to the temporarily open waters of Ouart Fotou valley, Ekia wadi and Karouassa valley. High σ_0 values are observed over wide portions of the latitudinal transect for several annual cycles. They can be related to rainfall events affecting the whole or large parts of the Gourma region as for example the strong rainfalls that occurred on August 11th, 2006 simultaneously with ENVISAT cycle 50 and the rainfall on June 26th, 2009 a few hours before ENVISAT cycle 80.

Besides, locally harsh topography affects data availability. The retracking algorithms based on modeling of the surface response (Ice-2 and Ocean) are unable to provide valid data over the erosion surface at 15.15° of latitude, and at the vicinity of the Hombori mounts (15.3° of latitude). This is likely due to the inability to fit the parameters of theoretical waveforms on the observed ones

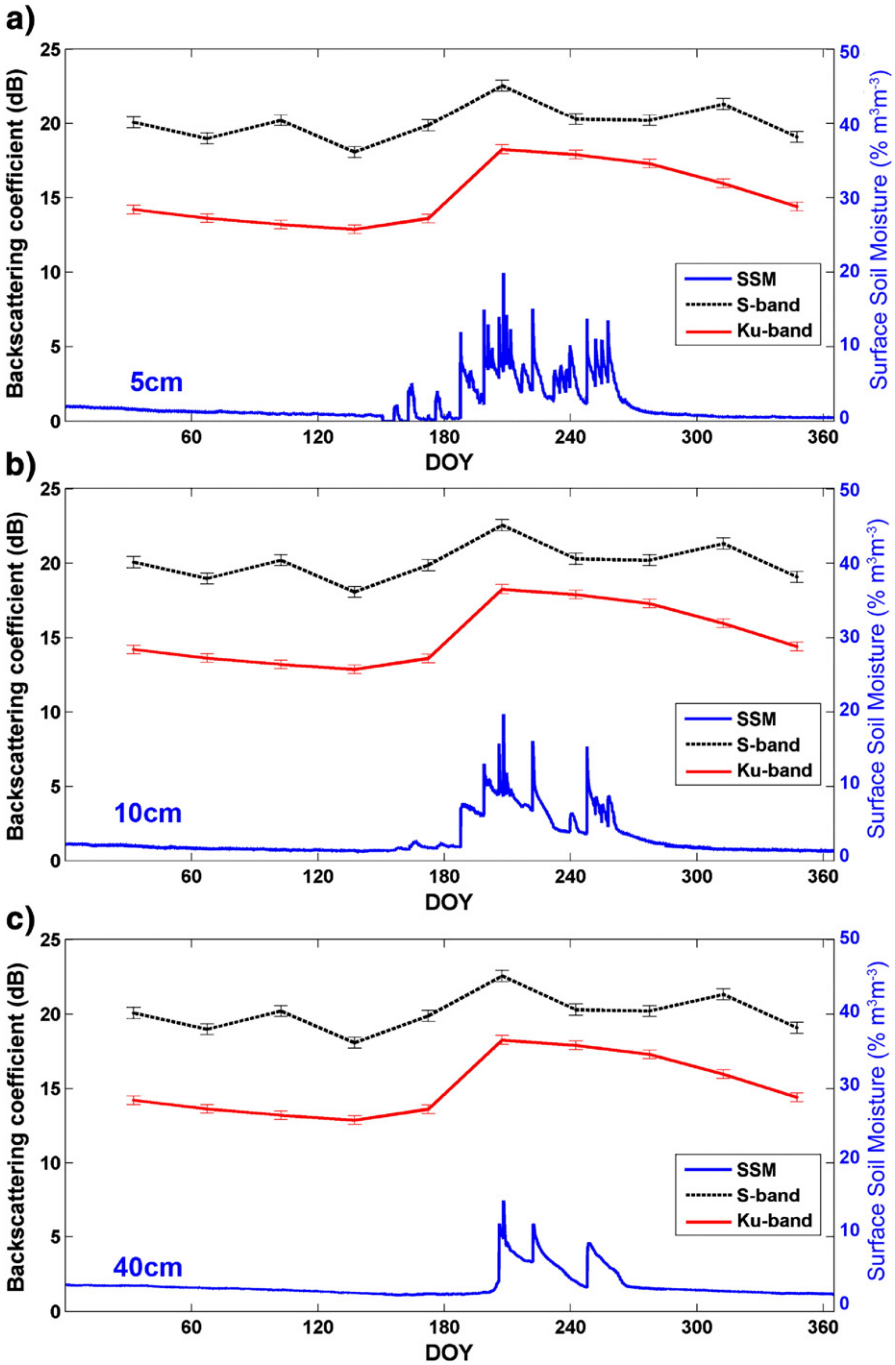

Fig. 4. Time variation of volumetric soil moisture in % (–), and Ice-1 algorithm backscattering coefficient σ_0 in dB for S-band (---) and Ku-band (–) at Agoufou site for year 2007. a) Soil moisture measurements at 5 cm depth; b) Soil moisture measurements at 10 cm depth and c) soil moisture measurements at 40 cm depth.

Table 4
Correlation coefficient (r) and Root Mean Square Error (RMSE) between in-situ measurement of surface soil moisture and S-band backscattering coefficients for the study sites.

Site		Agoufou			Bangui Mallam			Ekia			Kyrnia		
Period		2005–2007			2005–2007			2005–2007			2007		
Mean distance(km)		3			9.5			5.5			3		
SSM depth (cm)		5	10	40	5	10	30	5	10	30	5	10	30
Ice-1	N	25	25	25	20	20	20	22	22	22	8	8	8
	r	0.50*	0.41*	0.43*	0.64**	0.73**	0.40	0.70**	0.82**	0.80**	0.68	0.94**	0.98**
	RMSE (%)	3.87	6.34	4.97	4.52	3.28	6.77	2.62	1.93	2.14	4.44	1.98	1.34
Ice-2	N	24	24	24	20	20	20	22	22	22	8	8	8
	r	0.68**	0.66**	0.70**	0.75**	0.62**	0.58**	0.73**	0.83**	0.80**	0.76*	0.97**	0.99**
	RMSE (%)	2.4	3.27	2.41	3.37	4.35	4.11	2.41	1.87	2.13	3.54	1.29	0.78
Ocean	N	26	26	26	21	21	21	23	23	23	8	8	8
	r	0.27	0.36	0.41*	0.65*	0.64**	0.34	0.55**	0.70**	0.70**	0.73*	0.96**	0.99**
	RMSE (%)	7.94	7.37	5.19	4.36	4.12	7.88	3.93	2.77	2.86	3.96	1.55	0.84

* Significance >95%.
** Significance >99%.

whereas the empirical retracking processes (center of gravity for Ice-1 and maximum for Sea Ice of the waveform) are more robust.

4. Surface soil moisture estimation

4.1. Relationship between backscattering coefficient and SSM

In this section, the time variation of RA backscattering coefficients at the vicinity of the 6 in situ soil moisture stations (Ekia, Eguerit, Bangui Mallam, Agoufou, Kyrnia and Kobou) are analyzed and compared to the temporal variation of SSM measured in situ.

Two methods are used to build time series of backscattering coefficients at the vicinity of a ground soil moisture station. The first approach is based on the definition of a rectangular window of a few kilometers width around the nominal altimeter track corresponding to an area homogeneous in soil texture and topography. To obtain the backscattering coefficients time series, all the measurements that fall within this window are averaged for each cycle. This method is similar to the one used to derive water levels of rivers and lakes from radar altimetry data (e.g. Frappart et al., 2006a). The second approach consists in selecting the backscattering coefficient data the closest from the soil moisture site. However, at Ekia site (see Fig. 1 and Table 1), the selected data are the closest from a location 7 km to the South-west of the site instead, in order to minimize the effect of the presence of a temporary pond northward of the soil moisture site. The results presented below are obtained using the second approach that provides better results (i.e. higher correlation and lower RMSE).

The backscattering coefficients for Ku- and S-bands display a strong seasonality. Maxima of σ_0 are observed during the peak of the rainy season in close relation with SSM content measured at 5 and 10 cm depths, as illustrated for the Agoufou site for the Ice-1 algorithm (Fig. 4).

Rainfall events (not shown in Fig. 4) trigger an increase of SSM and as a consequence, an increase of the backscattering coefficient. The stronger the rainfall, the larger the response of the surface is. The variations of σ_0 during the dry season (<2 dB in Ku band and <3 dB in S band) can be related to instrumental noise and changes in the sampled surface caused by variations around the nominal track of the satellite. The variations over time of Ku-band σ_0 calculated with the Ice-1 retracking algorithm are compared to the variations of SSM measured at 5 cm depth for the different SSM sites. The yearly amplitudes of Ku-band σ_0 i.e. the difference in dB between the highest and lowest observed backscattering values vary from 4 to 20 dB, the highest values corresponding to the wettest years when in situ SSM is maximum. Although the seasonal σ_0 variations exhibit similar amplitudes across different sites, backscattering absolute values differ from one site to another. This may be caused by the heterogeneity of landscapes, the dispersion of radar measurements along the satellite track, and the presence of surface water. Higher correlations (by at least 0.15) between σ_0 and SSM are found when the closest σ_0 data to the soil moisture sites are selected rather than when

Table 5
Correlation coefficient (r) and Root Mean Square Error (RMSE) between in-situ measurement of surface soil moisture and Ku-band backscattering coefficients for the study sites.

Site		Agoufou			Bangui Mallam			Eguerit	Ekia			Kobou			Kyrnia		
Period		2005–2010			2005–2010			2008–2009	2005–2010			2008–2010			2007–2010		
Mean distance (km)		3			9.5			2	5.5			9.7			3		
SSM depth (cm)		5	10	40	5	10	30	5	5	10	30	5	10	30	5	10	30
Number of samples		56	56	56	27	49	49	13	51	51	51	28	28	28	29	29	29
Ice-1	r	0.85 **	0.85 **	0.55 **	0.7 **	0.73 **	0.3 *	0.95 **	0.59 **	0.63 **	0.55 **	0.52 **	0.33	0.54 **	0.66 **	0.66 **	0.6 **
	RMSE (%)	1.74	1.85	3.29	3.61	3.22	8.35	1.98	3.32	2.84	3.65	5.84	10.8	4.61	4.59	5.09	6.26
Ice-2	r	0.83 **	0.86 **	0.54 **	0.7 **	0.73 **	0.26	0.94 **	0.59 **	0.61 **	0.52 **	0.55 **	0.36	0.54 **	0.66 **	0.64 **	0.52 **
	RMSE (%)	1.85	1.76	3.4	3.54	3.23	9.67	2.36	3.33	2.99	3.94	5.34	10.03	4.66	4.51	5.38	7.79
Sea Ice	r	0.82 **	0.83 **	0.54 **	0.69 **	0.73 **	0.3 *	0.95 **	0.58 **	0.63 **	0.55 **	0.52 **	0.33	0.55 **	0.64 **	0.64 **	0.59 **
	RMSE (%)	1.9	2.02	3.4	3.66	3.19	8.32	2	3.44	2.86	3.61	5.8	10.83	4.55	4.78	5.35	6.53
Ocean	r	0.52 **	0.54 **	0.34 **	0.62 **	0.71 **	0.23	0.95 **	0.46 **	0.54 **	0.56 **	0.55 **	0.39 *	0.58 **	0.53 **	0.49 **	0.45 *
	RMSE (%)	4.52	4.63	5.89	4.38	3.41	11.12	2.05	4.74	3.65	3.6	5.35	8.85	4.25	6.44	8	9.29

* Significance >95%.
** Significance >99%.

several measurements are averaged over a given window. Correlation coefficients (r) and RMSE obtained by linear regression between both bands backscattering coefficients and SSM are presented in Table 4 for S-band and Table 5 for Ku-band. If the sites with a small number of observations (Eguerit and Kyrnia at S-band) are excluded, both frequencies show similar results with higher correlation found for Agoufou (at 5 and 10 cm) at Ku-band and Ekia (at 10 and 30 cm) at S-band. Since the period of observations is longer at Ku-band (~8 years) than at S-band (~5 years), in the following, analysis are performed only with the measurements acquired at Ku band (Fig. 5).

A very good agreement is found for the sites presenting homogeneous surface conditions within the altimeter footprint. For instance, the Agoufou and Bangui Mallam sites are located in large fixed sandy dunes with low and gentle elevation changes (a few meters). The closer to the ENVISAT track the measurements site, the better the correlation is. Correlation coefficients of 0.95 and 0.86 and RMSE of 1.98% and 1.74% are obtained between 5 cm depth SSM and Ice-1 estimated σ_0 for short distances of 2–3 km (Eguerit and Agoufou) whereas correlation coefficients (RMSE) range from 0.7 to 0.52 (3.61% to 5.84%) for distances larger than 5.5 km (Bangui Mallam, Ekia and Kobou). The poor results obtained at the Kyrnia site located at only 3 km from the altimeter swath are likely due to the presence of a temporary pond close to the site. Overall, the results are quite similar for SSM measured at 5 and 10 cm depth, as a mark of the soil moisture homogeneity close to soil surface. Similar results are found with Ice-2 and Sea Ice based σ_0. Overall, lower performances are obtained for Ocean processed data as no high frequency data (18 Hz) are available.

Scatterplots of backscattering coefficients as a function of measured SSM (Fig. 6) sometimes display very high values of σ_0

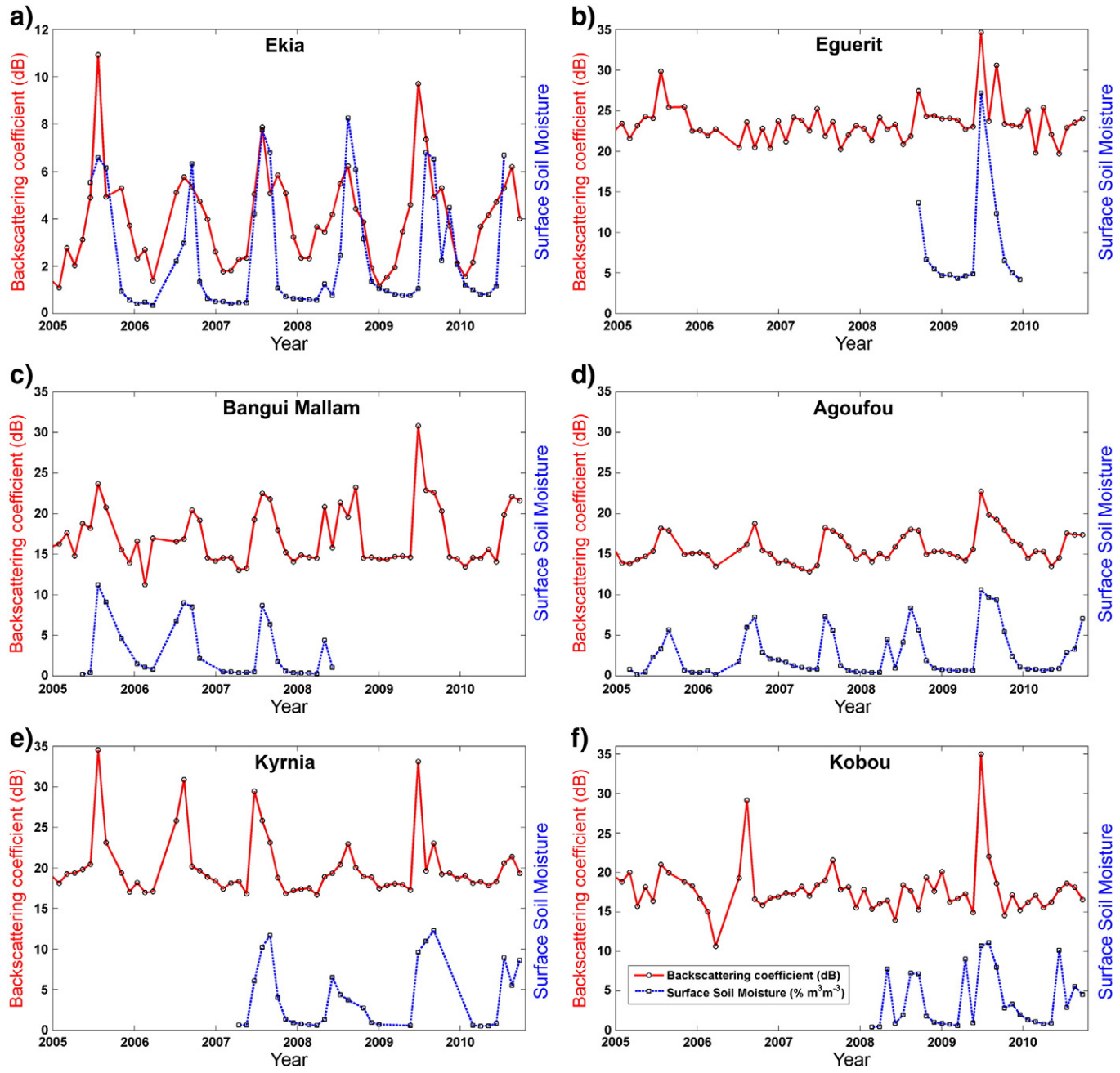

Fig. 5. Temporal variations of Ku-band Ice-1 backscattering coefficient σ_0 (__) in dB and volumetric soil moisture (SSM in %) at 5 cm depth (---) over the period January 2005 - October 2010. a) Ekia; b) Eguerit; c) Bangui Mallam; d) Agoufou; e) Kyrnia; f) Kobou.

(>30 dB) that do not correspond to high SSM measured in situ (see for example Fig. 6e–f). These off layers can be related to strong rainfall events that took place a couple of hours before the altimeter overpass (e.g. on June 26th, 2009) generating temporary puddles that enhanced the radar signal. In the case of Bangui Mallam, in situ soil moisture measurements are not available after mid-July 2008 at 5 cm depth.

4.2. Effect of seasonal dynamics of vegetation on SSM estimation

To determine whether the presence of vegetation affects the SSM–σ_0 relationships the variation of Ice-1 estimated σ_0 is plotted against the measured Leaf Area Index (LAI) during the 2005–2010 growing seasons for the Agoufou site. Methodology of LAI in situ measurements are detailed in Mougin et al. (submitted for publication). The maximum corresponding herbaceous vegetation cover at the Agoufou site is about 50%.

For LAI>0.2, the backscattering coefficient decreases (<2 dB) as the LAI increases with a correlation coefficient of −0.6 suggesting a weak attenuation of the radar wave by the vegetation layer. The impact of vegetation remains anyway small because (i) the radar altimeter is a nadir-looking instrument which means that the electromagnetic field crosses less vegetation (smaller canopy optical thickness) than side-looking radars (SAR or scatterometer) that

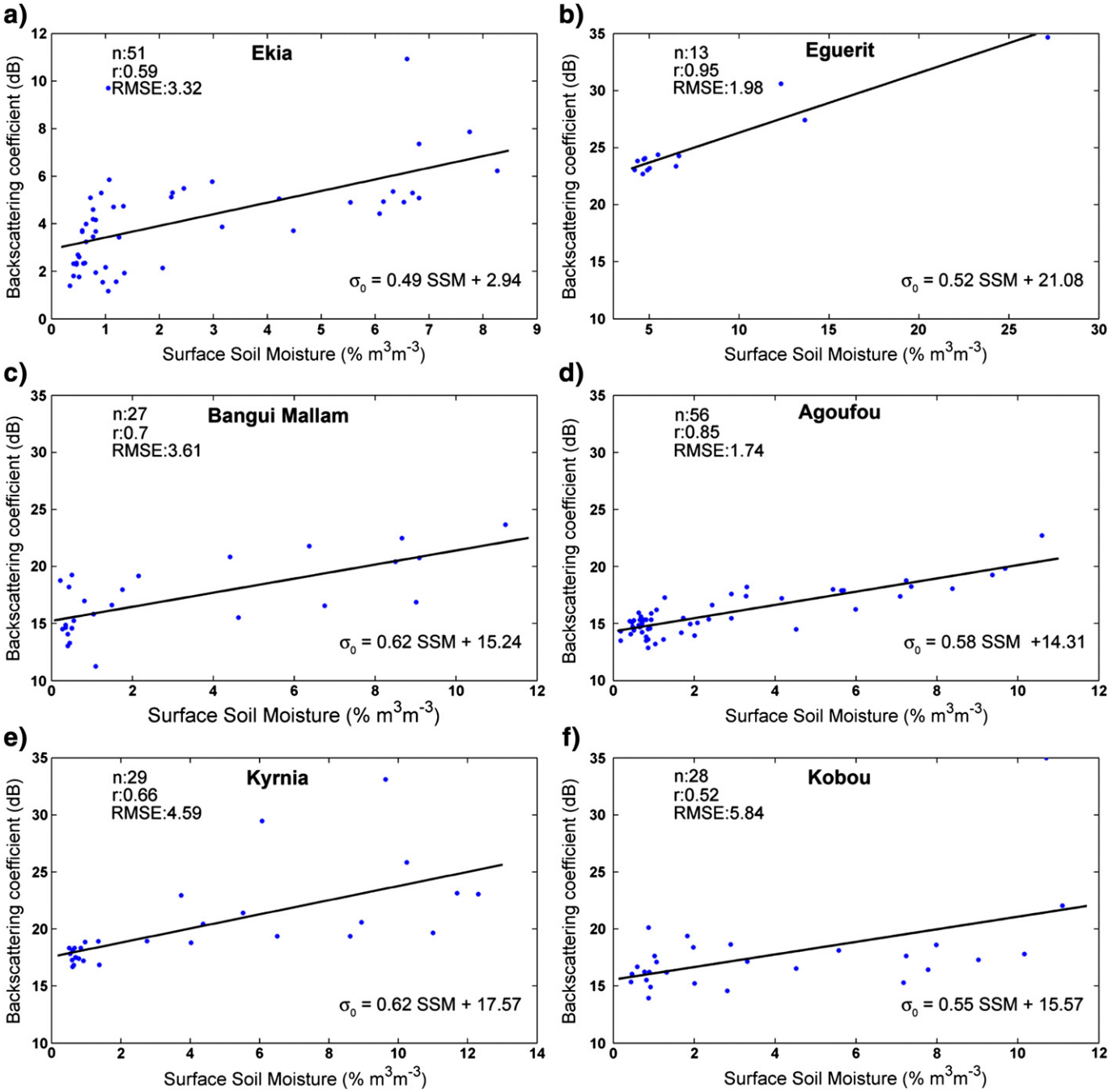

Fig. 6. Scatterplot of Ku-band Ice-1 backscattering coefficient σ_0 (in dB) versus volumetric soil moisture (SSM in %) at 5 cm depth. Correlation coefficient (r), Root Mean Square Error (RMSE) in % of soil moisture, and number of data (n) are also indicated. a) Ekia; b) Eguerit; c) Bangui Mallam; d) Agoufou; e) Kyrnia; f) Kobou.

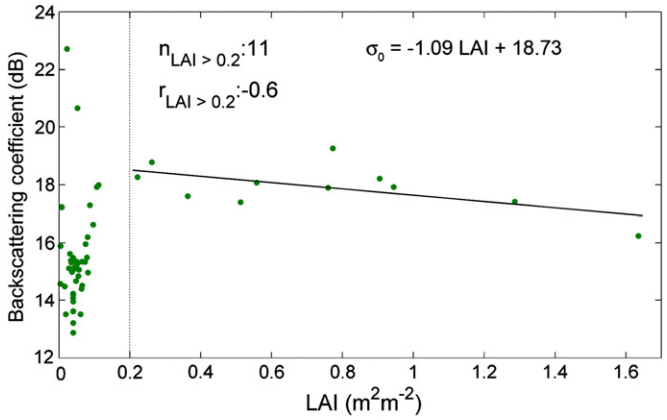

Fig. 7. Scatterplot of backscattering coefficient σ_0 (Ice-1 algorithm) versus Leaf Area Index (LAI) for the Agoufou site. Correlation coefficients (r) and number of samples (n) for LAI > 0.2 are given for the period 2005–2010. The linear equation is indicated.

observe the surface at angles greater than 10°, (ii) the Sahelian vegetation cover remains low even at the peak of the wet season (except in seasonally flooded forests that are not considered here) (Fig. 7).

For low LAI (LAI < 0.2) the observed increase of the backscattering coefficient with LAI could be attributed to an enhancement of the scattering by the vegetation layer as already observed on crops by Ulaby et al. (1984).

4.3. Linear regression and SSM estimation

Based on the experimental relationships displayed in Fig. 6, a general linear regression is established between normalized σ_0 and SSM for the sandy soils dominant across the Gourma mesoscale window (58% of the whole surface). Coefficients of the linear regression between normalized backscattering coefficients and in situ SSM measurements for the three sandy sites (Agoufou, Bangui Mallam and Ekia,) are determined and averaged (Fig. 8). Following the methodology proposed by Wagner and Scipal (2000) and Zribi et al. (2007), the normalized backscattering coefficients is calculated as the difference between the actual backscattering value and the mean backscattering value estimated over the core of the dry season (January to April) for each site. Indeed, the normalized backscattering coefficients reflect the radar dynamics of the different surface types.

Finally, altimeter-derived SSM time series are estimated by inverting the general linear relationship between backscattered and SSM established on sandy soils, for both 5 cm and 10 cm depths.

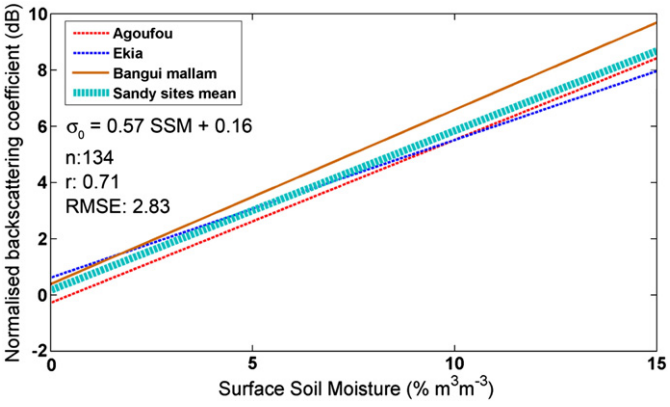

Fig. 8. Linear regression of the Ice-1 normalized backscattering coefficient σ_0 versus volumetric soil moisture at 5 cm for the sandy sites. The mean sandy site regression equation is indicated, along with the number of samples considered (n), the correlation coefficient (r) and the Root Mean Square Error (RMSE) given in % of soil moisture.

Table 6
Correlation coefficient (r) and Root Mean Square Error (RMSE) between in-situ measurement of surface soil moisture and Ku-band altimetry-derived surface soil moisture estimation for the 3 sandy sites of Agoufou, Bangui Mallam and Ekia.

Site		Agoufou		Bangui Mallam		Ekia	
In-situ SSM measurement depth (cm)		5	10	5	10	5	10
Ice-1	r	0.88**	0.87**	0.72**	0.73**	0.73**	0.64**
	RMSE (%)	1.39	1.50	3.29	3.79	2.26	2.33
Ice-2	r	0.86**	0.88**	0.76**	0.73**	0.74**	0.64**
	RMSE (%)	1.62	1.53	2.35	2.93	2.40	2.70
Sea Ice	r	0.87**	0.85**	0.71**	0.74**	0.72**	0.66**
	RMSE (%)	1.44	1.58	3.03	3.36	2.22	2.21
Ocean	r	0.69**	0.68**	0.65**	0.71**	0.49**	0.54**
	RMSE (%)	3.15	3.26	2.76	2.52	3.16	2.99*

* Significance > 95%.
** Significance > 99%.

Comparisons between in situ and altimetry-derived SSM are analyzed for the sandy sites using the four retracking algorithms. Results of these comparisons (RMSE and correlation coefficients) are summarized in Table 6 and an example of time series of altimetry-derived SSM is given for the Agoufou site (Fig. 9). The error introduced by the inverse function in the SSM derived from σ_0 is 0.4% SSM obtained as the ratio between the error on σ_0 (maximum value of 0.3 dB according to Pierdicca et al., 2006) and the slope of the mean linear regression.

4.4. Comparisons with ASCAT-derived SSM estimates

To compare the ASCAT derived SSM products at a resolution of 35 km to the ENVISAT RA-2 derived estimates, correlation coefficients have been calculated. For each product, the reference point is the location of the in-situ measurement site. Hence the ASCAT-derived SSM chosen for each study site is the one of the pixel containing the reference point. Outliers in the ASCAT-derived SSM are filtered out using a threshold of 30% of SSM. All the values of ENVISAT RA-2 derived SSM that fall within the ASCAT pixel corresponding to the site (see Section 4.1) are averaged. Consequently, at a given time, between 80 and 100 backscattering coefficients are taken into account. The acceptable time offset between ASCAT measurements and ENVISAT RA-2 data has been limited to 18 h.

Comparisons between altimetry derived SSM (for both 5 cm and 10 cm inverse functions) and ASCAT SSM products are performed

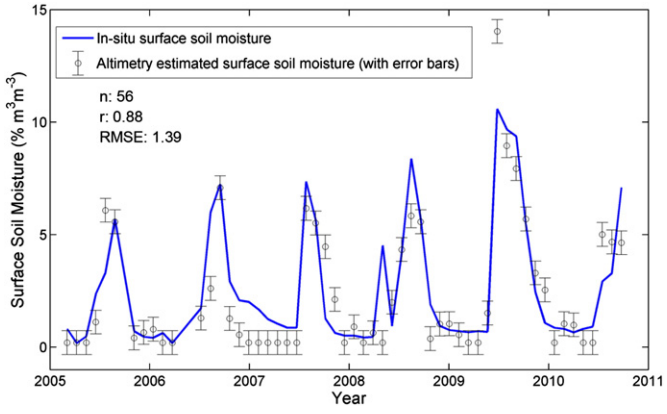

Fig. 9. Time variation of the volumetric soil moisture at Agoufou, measured at 5 cm depth (plain line) and estimated (circles with error bars) using the general σ_0–SSM relationships for sandy soils for Ice-1 backscattering coefficients. Are also indicated the number of samples considered (n), the correlation coefficient (R) and the Root Mean Square Error (RMSE) given in % of soil moisture.

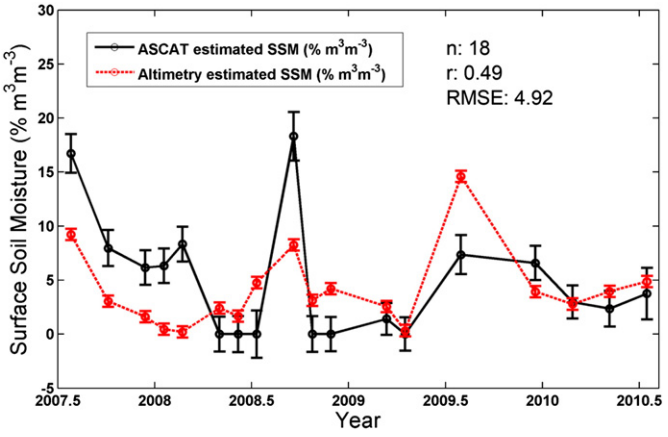

Fig. 10. Time variation of ASCAT SSM product and ENVISAT Ice-1 SSM estimation for the Agoufou site from 2007 to 2010, with the corresponding error bars. Are also indicated the number of samples considered (n), the correlation coefficient (r) and the Root Mean Square Error (RMSE) given in % of soil moisture.

for the measurements sites of Agoufou, Bangui Mallam, and Ekia. For the Agoufou site the time series are established from May 2007 to October 2010 (Fig. 10), the common period of availability of the ASCAT and ENVISAT data. The altimetry-derived SSM averaged over the ASCAT pixel exhibit similar temporal variations in phase with ASCAT-based SSM but with large difference of amplitudes reaching up to 12% $m^3\ m^{-3}$ of SSM. The correlation coefficients and RMSE calculated between the four different altimetry-based and ASCAT-derived SSM for the three selected sites (Table 7) exhibit large variations from one region to another with correlations around 0.5 for Agoufou, 0.4–0.5 for Ekia and only 0.3–0.4 for Bangui Mallam, and RMSE lower than 5% except at Ekia. These discrepancies can be accounted for the widely different scales observed by each sensor. ASCAT-based estimates are representative of larger areas (~1200 km²) than ENVISAT-derived SSM (~250 km²) using the ENVISAT integration over the ASCAT pixel.

5. Conclusion

This study has shown that backscattering coefficients at Ku-obtained from ENVISAT RA-2 data can be related to the temporal variation of moisture content in the upper soil profile. In situ SSM measurements and backscattering coefficients have been found generally well correlated, even if the quality of the relationships highly depends on i) the distance between the measurement site and the altimeter track, ii) the presence of open water in the altimeter footprint, iii) the topography of the site and the retracking algorithm. The best results are obtained for backscattering coefficients processed with Ice-1, Ice-2, and Sea-Ice algorithms compared to the Ocean retracking algorithm as no 20 Hz measurements are available with the latter one. A linear relationship between radar altimetry backscattering coefficients and SSM is established for the dominant sandy sites, similar to the ones previously found using ENVISAT-ASAR data over the same study area (see Baup et al., 2007, 2011). Only a small attenuation by the vegetation cover is found allowing SSM to be accurately estimated from radar altimetry data without any correction. To our knowledge, this is the first demonstration of the potentialities of radar altimetry to derive surface soil moisture in a semi-arid environment.

Comparisons of altimetry derived SSM with low spatial resolution SSM products obtained from ASCAT scatterometer data show reasonable correlation between the two satellite-derived estimates. Radar altimetry-based SSM products offer new and complementary information to relate the local (in situ) to the regional (~25 km) scales, and demonstrate a strong potential to evaluate low resolution satellite SSM products to be used in a down-scaling approach.

Improvements of altimetry derived SSM are expected from the use of higher spatial resolution altimetry data such as those that will be provided by the French-Indian AltiKa radar altimetry mission to be launched in August 2012.

Table 7
Correlation coefficients (r), bias and RMSE between ASCAT SSM products and RA-2 Ku-band derived SSM for 3 study sites (Agoufou, Bangui-Mallam and Ekia).

Site		Agoufou		Bangui Mallam		Ekia	
Inversion function (depth in cm)		5	10	5	10	5	10
Ice-1	r	0.49*	0.47*	0.30	0.30	0.42	0.43
	RMSE (%)	4.92	4.92	4.04	3.95	10.41	9.25
	bias	0.9062	0.72	−0.90	−1.18	−8.01	−6.77
Ice-2	r	0.56*	0.54*	0.39	0.39	0.48*	0.48*
	RMSE (%)	4.59	4.67	3.70	3.65	7.98	7.45
	Bias	1.48	1.09	−0.99	−1.46	−6.97	−6.56
Sea Ice	r	0.49*	0.47*	0.30	0.30	0.43	0.43
	RMSE (%)	4.89	4.91	3.99	3.91	9.83	8.79
	Bias	0.91	0.69	−0.99	−1.29	−7.35	−6.31
Ocean	r	0.50*	0.50*	0.29	0.29	0.45	0.45
	RMSE (%)	4.82	4.83	3.72	3.71	5.45	5.43
	Bias	0.3135	−0.0865	−1.21	−1.64	−4.51	−4.78**

* Significance > 95%.
** Significance > 99%.

Acknowledgments

This work was performed within the framework of the AMMA project. Based on a French initiative, AMMA has been constructed by an international group and is currently funded by large number of agencies, especially from France, the UK, the US and Africa. It has been the beneficiary of a major financial contribution from the European Community's Sixth Framework Research Programme. Detailed information on the scientific coordination and funding is available on the AMMA international web site (https://www.amma-eu.org/). This work was funded by the Programme National en Télédétection Spatiale (PNTS) in the framework of the project "Potentialités des altimètres radars spatiaux pour l'hydrologie en zone sahélienne. Perspectives pour la mission SWOT".

The authors thank the Centre de Topographie des Océans et de l'Hydrosphère (CTOH) at Laboratoire d'Etudes en Géophysique et Océanographie Spatiales (LEGOS), Observatoire Midi-Pyrénées (OMP), Toulouse, France for providing the ENVISAT RA-2 GDR dataset used in the present study.

References

Bamber, J. L. (1994). Ice sheet altimeter processing scheme. *International Journal of Remote Sensing, 15*(4), 925–938.
Baup, F., Mougin, E., de Rosnay, P., Hiernaux, P., Frappart, F., Frison, P. L., et al. (2011). Mapping surface soil moisture over the Gourma mesoscale site (Mali) by using ENVISAT-ASAR data. *Hydrology and Earth System Sciences, 15*, 603–616.
Baup, F., Mougin, E., de Rosnay, P., Timouk, F., & Chênerie, I. (2007). Surface soil moisture estimation over the AMMA Sahelian site in Mali using ENVISAT/ASAR data. *Remote Sensing of Environment, 109*(4), 473–481.
Birkett, C. M. (1995). The contribution of TOPEX/POSEIDON to the global monitoring of climatically sensitive lakes. *Journal of Geophysical Research, 100*(C12), 25,179–25,204.
Birkett, C. M. (1998). Contribution of the TOPEX NASA radar altimeter to the global monitoring of large rivers and wetlands. *Water Resources Research, 34*(5), 1223–1239.
Birkett, C. M., Mertes, L. A. K., Dunne, T., Costa, M. H., & Jasinski, M. J. (2002). Surface water dynamics in the Amazon basin: Application of satellite radar altimetry. *Journal of Geophysical Research, 107*(D20), 8059–8080.
Bramer, S. M. S., Berry, P. A. M., & Carter, J. (2010). The use of radar altimetry in soil moisture monitoring in support of the SMOS mission. *Proceedings of Earth Observation and Water Cycle Science, Frascati, Italy, 18–20 November 2009 (ESA SP-674, January 2010)*.
Brown, G. S. (1977). The average impulse response of a rough surface and is applications. *IEEE Transactions on Antennas and Propagation, 25*(1), 67–74.
Brümmer, C., Falk, U., Papen, H., Szarzynski, J., Wassmann, R., & Brüggemann, N. (2008). Diurnal, seasonal, and interannual variation in carbon dioxide and energy

exchange in shrub savanna in Burkina Faso (West Africa). *Journal of Geophysical Research*, *113*, G02030, http://dx.doi.org/10.1029/2007JG000583 11 pp.
Cazenave, A., Bonnefond, P., & Do Minh, K. (1997). Caspian sea level from Topex/Poseidon altimetry: Level now falling. *Geophysical Research Letters*, *25*(2), 155–158.
Chelton, B. C., Ries, J. C., Haines, B. J., Fu, L., & Callahan, P. S. (2001). Satellite altimetry. In L. Fu, & A. Cazenave (Eds.), *Satellite Altimetry and Earth Sciences: An Handbook of Techniques and Applications* (pp. 1–131). : Academic Press.
Crétaux, J. F., Calmant, S., Romanovski, V., Shibuyin, A., Lyard, F., Berge-Nguyen, M., et al. (2009). An absolute calibration site for radar altimeters in the continental domain: Lake Issykkul in Central Asia. *Journal of Geodesy*, *83*(8), 723–735.
Cudlip, W., Ridley, J. K., Strawbridge, F., Harris, A., & Rapley, C. G. (1994). Detecting surface roughness and moisture variations in deserts. *Proceedings of the 2nd ERS-1 Symposium, Hamburg 1993, ESA SP-361* (pp. 849–853).
de Rosnay, P., Gruhier, C., Timouk, F., Baup, F., Mougin, E., Hiernaux, P., et al. (2009). Multi-scale soil moisture measurements over the Gourma meso-scale site in Mali. *Journal of Hydrology*, *375*(1–2), 241–252 (AMMA CATCH special issue).
ESA (2002). *ENVISAT RA2/MWR Product handbook*. RA2/MWR products user guide.
Frappart, F., Calmant, S., Cauhopé, M., Seyler, F., & Cazenave, A. (2006). Preliminary results of ENVISAT RA-2-derived water levels validation over the Amazon basin. *Remote Sensing of Environment*, *100*(2), 252–264, http://dx.doi.org/10.1016/j.rse.2005.10.027.
Frappart, F., Do Minh, K., L'Hermitte, J., Cazenave, A., Ramillien, G., Le Toan, T., et al. (2006). Water volume change in the lower Mekong from satellite altimetry and imagery data. *Geophysical Journal International*, *167*(2), 570–584, http://dx.doi.org/10.1111/j.1365246X.2006.03184.x.
Frappart, F., Hiernaux, P., Guichard, F., Mougin, E., Kergoat, L., Arjounin, M., et al. (2009). Rainfall regime over the Sahelian climate gradient in the Gourma, Mali. *Journal of Hydrology*, *375*(1–2), 128–142 (AMMA CATCH special issue).
Frappart, F., Seyler, F., Martinez, J. -M., Leon, J. -G., & Cazenave, A. (2005). Floodplain water storage in the Negro River basin estimated from microwave remote sensing of inundation area and water levels. *Remote Sensing of Environment*, *99*(4), 387–399.
Hayne, G. S. (1980). Radar altimeter mean return waveforms from near normal-incidence ocean surface scattering. *IEEE Transactions on Antennas and Propagation*, *28*(5), 687–692.
Hiernaux, P., Mougin, E., Diarra, L., Soumaguel, N., Lavenu, F., Tracol, Y., et al. (2009). Rangeland response to rainfall and grazing pressure over two decades: herbaceous growth pattern, production and species composition in the Gourma, Mali. *Journal of Hydrology*, *375*, 114–127.
Koster, R. D., Dirmeyer, P., Guo, Z., Bonan, G., Cox, P., Gordon, C., et al. (2004). Regions of strong coupling between soil moisture and precipitation. *The Sciences*, *305*, 1038–1040.
Laxon, S. (1994). Sea ice altimeter processing scheme at the EODC. *International Journal of Remote Sensing*, *15*(4), 915–924.
Legrésy, B. (1995). Etude du retracking des surfaces des formes d'onde altimétriques au-dessus des calottes. *rapport CNES, CT/ED/TU/UD96.188, contrat n° 856/2/95/CNES/006* 81 pp.
Legrésy, B., Papa, F., Rémy, F., Vinay, G., van den Bosch, M., & Zanife, O. Z. (2005). ENVISAT radar altimeter measurements over continental surfaces and ice caps using the ICE-2 retracking algorithm. *Remote Sensing of Environment*, *95*, 150–163, http://dx.doi.org/10.1016/j.rse.2004.11.018.
Legrésy, B., & Rémy, F. (1997). Surface characteristics of the Antarctic ice sheet and altimetric observations. *Journal of Glaciology*, *43*(144), 197–206.
Mladenova, I., Lakshmi, V., Walker, J. P., Panciera, R., Wagner, W., & Doubkova, M. (2010). Validation of the ASAR Global Monitoring Mode Soil Moisture Product Using the NAFE'05 Data Set. *IEEE Transactions on Geoscience and Remote Sensing*, *48*, 2498–2508.
Moran, M. S., Hymer, D. C., Qi, J., & Sano, E. E. (2000). Soil moisture evaluation using-temporal synthetic aperture radar (SAR) in semiarid rangeland. *Agricultural and Forest Meteorology*, *105*, 69–80.
Mougin, E., Demarez, V., Hiernaux, P., Diawara, M., Berg, A. (submitted for publication). Estimation of LAI, fCover and fAPAR of a Sahelian grassland (Gourma, Mali). *Agricultural and Forest Meteorology*.
Mougin, E., Hiernaux, P., Kergoat, L., de Rosnay, P., Grippa, M., Timouk, F., et al. (2009). The AMMA-CATCH Gourma observatory site in Mali: Relating climate variations to changes in vegetation, surface hydrology, fluxes and natural resources. *Journal of Hydrology*, *375*(1–2), 14–33, http://dx.doi.org/10.1016/j.hydrol.2009.06.0045.
Naeimi, V., Scipal, K., Bartalis, Z., Hasenauer, S., & Wagner, W. (2009). An improved soil moisture retrieval algorithm for ERS and METOP scatterometer observations. *IEEE Transactions on Geoscience and Remote Sensing*, *47*(7), 1999–2013, http://dx.doi.org/10.1109/TGRS.20082011617.
Papa, F., Legrésy, B., & Rémy, F. (2003). Use of the Topex-Poseidon dual-frequency radar altimeter over land surfaces. *Remote Sensing of Environment*, *87*, 136–147, http://dx.doi.org/10.1016/S0034-4257(03)00136-6.
Peacock, N. R., & Laxon, S. W. (2004). Sea surface height determination in the Arctic Ocean from ERS altimetry. *Journal of Geophysical Research, Oceans*, *109*, C07001.
Pierdicca, N., Greco, B., Bignami, C., Ferrazzoli, P., Mattioli, V., & Pulvirenti, L. (2006). The calibration of the Envisat radar altimeter by a passive technique. *IEEE Transactions on Geoscience and Remote Sensing*, *44*(11), 3297–3307.
Redelsperger, J. -L., Thorncroft, C., Diedhiou, A., Lebel, T., Parker, D., & Polcher, J. (2006). African monsoon, multidisciplinary analysis (AMMA): An international research project and field campaign. *Bulletin of the American Meteorological Society*, *87*(12), 1739–1746.
Ridley, J., Strawbridge, F., Card, R., & Phillips, H. (1996). Radar backscatter characteristics of a desert surface. *Remote Sensing of Environment*, *57*(2), 63–78.
Santos da Silva, J., Calmant, S., Seyler, F., Rottuno Filho, O. C., Cochonneau, G., & Mansur, W. J. (2010). Water levels in the Amazon basin derived from the ERS 2 and ENVISAT radar altimetry missions. *Remote Sensing of Environment*, *114*(10), 2160–2181, http://dx.doi.org/10.1016/j.rse.2010.04.020.
Tansey, K. J., Millington, A. C., Battikhi, A. M., & White, K. H. (1999). Monitoring soil moisture dynamics using satellite imaging radar in northeastern Jordan. *Applied Geography*, *19*, 325–344.
Taylor, C. T., Harris, P. P., & Parker, D. J. (2010). Impact of soil moisture on the development of a Sahelian mesoscale convective system: a case-study from the AMMA Special Observing Period. *Quarterly Journal of the Royal Meteorological Society*, *136*, 456–470.
Ulaby, F. T., Allen, C. T., Eger, G., & Kanemasu, E. (1984). Relating the microwave backscattering coefficient to Leaf Area Index. *Remote Sensing of Environment*, *14*, 113–133.
Ulaby, F. T., Fung, A. K., & Moore, R. K. (1981). *Microwave and remote sensing active and passive*. Norwood, MA: Artech House.
Wagner, W. (1998). *Soil moisture retrieval from ERS scatterometer data*. PhD dissertation, Institute for Photogrammetry and Remote Sensing, Vienna, University of Technologu, 111 pp.
Wagner, W., & Scipal, K. (2000). Large-scale Soil moisture mapping in western Africa using the ERS Scatterometer. *IEEE Transactions on Geoscience and Remote Sensing*, *38*, 1777–1782.
Wehr, T., & Attema, E. (2001). Geophysical validation of ENVISAT data products. *Advances in Space Research*, *28*(1), 83–91.
Wingham, D. J., Rapley, C. G., & Griffiths, H. (1986). New techniques in satellite altimeter tracking systems. *Proceedings of IGARSS'86 Symposium, Zürich, 8–11 Sept. 1986, Ref. ESA SP-254* (pp. 1339–1344).
Zech, W., Senesi, N., Guggenberger, G., Kaiser, K., Lehmann, J., Miano, T. M., et al. (1997). Factors controlling humification and mineralization of soil organic matter in the tropics. *Geoderma*, *79*(1–4), 117–161.
Zelli, C. (1999). ENVISAT RA-2 advanced radar altimeter: Instrument design and pre-launch performance assessment review. *Acta Astronautica*, *44*, 323–333.
Zribi, M., Andre, C., Saux-Picard, S., Descroix, L., Otlle, C., & Kallel, A. (2007). Soil moisture mapping based on ASAR/ENVISAT radar data over a Sahelian region. *International Journal of Remote Sensing*, *29*, 3547–3565.